

Steady-state space-charge-limited current analysis of mobility with negative electric field dependence

Gyanendra Bhattarai, Anthony N. Caruso, and Michelle M. Paquette^{a)}

Department of Physics and Astronomy, University of Missouri-Kansas City, Kansas City, Missouri 64110, USA

(Received 3 May 2018; accepted 2 July 2018; published online 23 July 2018)

We revisit the theory of steady-state space-charge-limited current (SS-SCLC) enhanced by Frenkel emission originally addressed by Murgatroyd using analytical rather than numerical integration to obtain an exact solution. For the first time, the analysis is also extended to the case of mobility exhibiting negative field dependence, generally observed in disordered materials at lower electric field. For the case of positive electric field dependence, we confirm that Murgatroyd's original solution is close to the exact solution for low and moderately high electric fields. At a very high field, the exact solution is consistent with the analytical solution given by Barbe. For the case of negative electric field dependence, the fit expression retains the same functional form as Murgatroyd's solution, however with a different exponential factor of -0.801 . The development of SS-SCLC theory for the case of negative field dependence is an important step in the generalization of this analysis technique to the investigation of complex materials such as disordered organic semiconductors.

Published by AIP Publishing. <https://doi.org/10.1063/1.5038578>

I. INTRODUCTION

The surge in popularity of thin-film organic electronics^{1–3} has spurred challenges in applying traditional analysis techniques to the measurement of charge transport properties in these materials. One charge transport parameter essential to performance in many devices is charge carrier mobility. Of the methods available for measuring mobility in low-mobility thin-film semiconductors, the steady-state space-charge-limited current (SS-SCLC) experiment stands out as arguably the most simple yet generally effective technique.⁴ This technique is based on the analysis of a current density vs voltage (J - V) curve of a sandwich thin-film structure and is amenable to screening a wide range of samples. Alternative transient, drift-mobility-based techniques, while potentially more appealing from a theory and accuracy standpoint, entail more elaborate experimental setups and maintain very specific requirements in terms of test heterostructure configuration (e.g., film thickness, contact type) and applicable charge transport property range,⁵ rendering them less versatile as a general measurement tool. Time-of-flight measurements, for example, require relatively thick ($>1\ \mu\text{m}$) films and transparent blocking contacts.^{5,6} Other techniques, including transient or dark-injection space-charge-limited current,⁷ charge extraction by linearly increasing voltage,⁸ and admittance spectroscopy,⁸ possess similarly exacting requirements to achieve successful measurements. Despite the relative simplicity and utility of the SS-SCLC technique, however, it is not without its challenges,⁴ including the appropriate treatment of samples exhibiting field-dependent mobility, as will be the focus of this work.

When an electric field is applied across an insulator (or insulating semiconductor), space-charge-limited conduction occurs when the injected carrier concentration exceeds the

thermal equilibrium concentration, leading to an excess of charge and non-uniform electric field profile across the film.⁹ The theory of space-charge-limited current (SCLC) was developed by Mott and Gurney¹⁰ for the case of a perfect crystalline trap-free insulator and has been revised by many authors.^{9,11} A quantum mechanical treatment of the space-charge-limited current has recently been described by González.¹² In the classical theory, the current density, J , through a single-carrier parallel-plate device is given by

$$J = \frac{9}{8} \epsilon \mu \frac{V^2}{d^3}, \quad (1)$$

where V is the applied voltage across the insulator, and d , ϵ , and μ are its thickness, permittivity, and charge carrier mobility, respectively. The SCLC theory has also been extended for the case of a single level of traps,⁹ where the current density is reduced by a factor θ

$$J = \frac{9}{8} \epsilon \mu \theta \frac{V^2}{d^3}. \quad (2)$$

Here, θ represents the ratio of free charge carrier concentration to total (free + trapped) charge carrier concentration. Additional treatments exist for more complex distributions of trap states.^{9,11}

Carrier mobility is typically extracted by fitting the experimental J - V data to Eq. (1) or (2). However, complications in data analysis arise when the carrier concentration and/or mobility exhibit an electric field dependence. One cause for such a dependence is the Poole-Frenkel effect,¹³ wherein an increase in the electric field lowers the effective trap depth, leading to an increase in free charge carriers and thus deviation from strict SCLC behavior. The ratio of free to total charge carriers then becomes

$$\theta = \theta_0 \exp(\beta \sqrt{E}) \quad (3a)$$

^{a)}Author to whom correspondence should be addressed. Electronic mail: paquettem@umkc.edu

with

$$\beta = \frac{1}{kT} \left(\frac{e^3}{\pi\epsilon} \right)^{\frac{1}{2}}. \quad (3b)$$

A well-known and often applied numerical solution for the space-charge-limited current density enhanced by Frenkel emission was reported by Murgatroyd¹⁴ as

$$J = \frac{9}{8} \epsilon \mu \frac{V^2}{d^3} \exp \left(0.891 \beta \sqrt{\frac{V}{d}} \right). \quad (4)$$

Although a complete analytical solution for the problem has not been obtained, analytical solutions with low-field ($\beta\sqrt{V/d} \ll 1$) and high-field ($\beta\sqrt{V/d} \gg 1$) approximations have been given by Barbe,¹⁵ and an exact but parametric solution has been reported by Bisquert *et al.*¹⁶

Exponential electric field dependence can also arise from the field dependence of the mobility related to the hopping transport of carriers in disordered materials,¹⁷ which takes on the same functional form as in the case of Frenkel emission

$$\mu(E) = \mu_0 \exp(\gamma\sqrt{E}). \quad (5)$$

Here, μ_0 is the low-field carrier mobility and γ is a fitting factor related to the material disorder. Although the factor γ is not necessarily equivalent to the Poole–Frenkel coefficient, β , this behavior is commonly referred to as Poole–Frenkel-like and the two treatments are often used interchangeably. An interesting experimental result^{18–24} obtained for a number of disordered organic semiconductors is a negative value of γ at low electric field, which cannot be explained on the basis of Frenkel emission. Although controversial,^{21,23,25} many have proposed, mostly based on numerical simulations, that under the Gaussian disorder model of hopping transport, this negative field dependence can result from the superposition of positional and energetic disorder in organic semiconductors.^{17,26,27} The functional form of the field-dependent mobility in this model is given as

$$\mu(T, E) = \mu_0 \exp \left(-\frac{2}{3} \hat{\sigma}^2 \right) \exp [C(\hat{\sigma}^2 - \Sigma^2)\sqrt{E}], \quad (6)$$

where $\hat{\sigma} = \sigma/k_B T$ is a measure of energetic disorder, with σ being the width of the Gaussian density of states, Σ is a measure of positional disorder, and C is a fitting parameter. This equation implies that when the positional disorder, Σ , exceeds the energetic disorder, $\hat{\sigma}$, particularly at high temperature, the mobility exhibits negative field dependence. The usual phenomenological explanation¹⁷ is that in three-dimensionally disordered systems with high positional disorder, the most energetically favorable path for percolative hopping transport will proceed via randomly oriented jumps; however, with increasing electric field, charge carriers are forced to make less energetically favorable jumps in the direction of the field, thus reducing mobility.

Although a negative field dependence for γ has been demonstrated in a number of different disordered materials using various transient mobility measurement techniques,^{18–22} we

are not aware of any reports of negative-field-dependent mobility based on SS-SCLC analysis. This lies in contrast to the case of positive-field-dependent mobility, which has been shown using both transient and steady-state measurements.²⁸

In principle, however, since all of the transient experiments used to determine carrier mobility require that the device under test be well into the space-charge-limited-current regime, the steady-state SCLC analysis should yield a negative field dependence for samples that present this behavior in the transient experiment. One reason for the lack of experimental SS-SCLC evidence for negative-field-dependent mobility may be a lack of theoretical framework. Although the numerical solution given by Murgatroyd [Eq. (4)] describes SS-SCLC with positive field dependence, to our knowledge, a solution for negative field dependence has not been reported, and one cannot simply apply Murgatroyd's treatment to this case. Here, we revisit a solution for the space-charge-limited current density incorporating the Poole–Frenkel or Poole–Frenkel-like effect for *both* positive and negative electric field dependence. In contrast to Murgatroyd's original solution, which uses numerical integration, this solution uses analytical integration. We compare our exact solution for the positive case to Murgatroyd's original solution as well as to Barbe's analytical solution for high field and discuss best practices for and implications of the SS-SCLC analysis for materials exhibiting negative-field-dependent mobility.

II. RESULTS AND DISCUSSION

For a single type of mobile carrier flowing through an insulator with field-dependent mobility given by Eq. (5), the total current through the insulator can be written as

$$J = \epsilon \mu_0 \exp \left(\gamma \sqrt{E(x)} \right) E(x) \frac{\partial E(x)}{\partial x} \quad (7)$$

with the charge density replaced by Poisson's equation

$$\nabla \cdot E = \frac{\rho(x)}{\epsilon}. \quad (8)$$

Here, the current due to the thermal equilibrium carrier concentration has been neglected. Equation (7) can also represent the case of space-charge-limited current enhanced by Frenkel emission. However, in this case, μ_0 represents $\mu\theta_0$ where θ_0 is given by Eq. (3a).

The solution of the continuity equation under steady-state conditions requires boundary conditions on the electric field. The usual consideration in the space-charge-limited current analysis is that the electric field at the injecting electrode ($x = 0$) is negligibly small because the electric field set up by the injected carriers opposes the applied electric field.¹⁰ Since the current density should remain constant spatially in the steady-state case, it is reasonable to solve the problem by direct integration of Eq. (7) with the boundary condition $E(0) = 0$, which gives

$$\frac{\gamma^4 J}{2\epsilon\mu_0} x = \exp \left(\gamma \sqrt{E(x)} \right) \left(\left(\gamma \sqrt{E(x)} \right)^3 - 3\gamma^2 E(x) + 6\gamma \sqrt{E(x)} - 6 \right) + 6. \quad (9)$$

It should be noted that for a real physical system, only the solution to Eq. (9) yielding positive $\sqrt{E(x)}$ should be chosen so that the field dependence in the carrier concentration [Eq. (3a)] and the carrier mobility [Eq. (5)] remain physically meaningful. For the case of negative field dependence (negative γ), the right-hand-side of the above equation saturates at 6 at high field, which in turn causes the current to saturate. However, in real devices, other high-field effects increase the current significantly and the high field saturation is not actually observed.

Because an analytical solution to Eq. (9) for $E(x)$ is not possible, we will proceed to a parametric solution following the method used by Murgatroyd. For this, we reduce Eq. (9) to a dimensionless format by defining some variables as

$$\text{Normalized current density: } \eta = \frac{2dJ\gamma^4}{\epsilon\mu_0}, \quad (10a)$$

$$\text{Normalized electric field: } z = \gamma^2 E, \quad (10b)$$

$$\text{Normalized thickness: } y = \frac{x}{d}, \quad (10c)$$

$$\text{Normalized voltage: } \xi = \frac{3V}{2d}\gamma^2, \quad (10d)$$

where V and d are the applied voltage and thickness of the device, respectively. With these variables defined, Eq. (9) takes the following form for positive field dependence:

$$\eta y = 24 + 4 \exp(\sqrt{z}) \left(z^{\frac{3}{2}} - 3z + 6\sqrt{z} - 6 \right). \quad (11a)$$

And for negative field dependence

$$\eta y = 24 - 4 \exp(-\sqrt{z}) \left(z^{\frac{3}{2}} + 3z + 6\sqrt{z} + 6 \right). \quad (11b)$$

In both equations, the variable \sqrt{z} is positive.

The applied voltage across an insulator of thickness d is obtained by integrating the electric field over the entire thickness as

$$V = \int_0^d E(x) dx, \quad (12)$$

which can easily be translated to the normalized form as

$$\xi = \frac{3}{2} \int_0^1 z dy. \quad (13)$$

The analytical solutions to Eqs. (11a) and (11b) give z as a function of ηy . Thus, it is reasonable to change the integral variable (y) in Eq. (13) to ηy . Since the normalized current (η) is a function of the normalized voltage (ξ), it is possible to write Eq. (13) as

$$\xi(\eta) = \frac{3}{2\eta} \int_0^\eta z(\eta y) d(\eta y). \quad (14)$$

As the closed form solutions of Eqs. (11a) and (11b) are not possible, the integral in Eq. (14) can be obtained as

$$\xi(\eta) = \frac{3}{2\eta} I \quad (15)$$

with

$$I = z_0 \eta - \int_0^{z_0} \eta y(z) dz, \quad (16)$$

where z_0 is the normalized electric field at the collecting electrode of the device ($y = 1$) where $\eta y = \eta$ (Fig. 1).

For positive field dependence, using Eq. (11a) for the expression of $\eta y(z)$, the integral I can be easily calculated to obtain (see the Appendix)

$$I = 4 \exp(\sqrt{z_0}) \left(z_0^{\frac{5}{2}} - 5z_0^2 \right) + 20\eta. \quad (17)$$

Hence, the normalized voltage $\xi(\eta)$ from Eq. (15) can be written as

$$\xi(\eta) = 30 + \frac{6 \exp(\sqrt{z_0}) \left(z_0^{\frac{5}{2}} - 5z_0^2 \right)}{\eta}. \quad (18)$$

Proceeding in a similar fashion to the above, we get the normalized voltage in the case of negative field dependence as

$$\xi(\eta) = 30 - \frac{6 \exp(-\sqrt{z_0}) \left(z_0^{\frac{5}{2}} + 5z_0^2 \right)}{\eta}. \quad (19)$$

Although z_0 cannot be solved for η analytically, it is possible to obtain the relation between the normalized current (η) and the normalized voltage (ξ) numerically. Since $\sqrt{z_0}$ is always positive as required for the field dependence, we can start with $z_0 = 0$ and calculate the normalized current (η) using Eqs. (11a) and (11b). Using Eqs. (18) and (19), the normalized voltage (ξ) can then be calculated. Although the process is numerical, the variation of the normalized current η as a function of normalized voltage ξ is exact. Thus, Eqs. (18) and (19) along with Eqs. (11a) and (11b) provide an exact solution for the space-charge-limited current for both positive as well as negative field dependence. For the positive field dependence case, the solution is equivalent to the parametric solution given by Bisquert *et al.*¹⁶

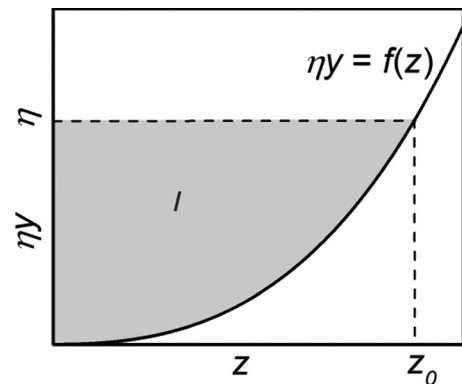


FIG. 1. Variation of ηy against the normalized electric field z for positive field dependence. The integral I (shaded portion) is obtained by subtracting the area of the unshaded portion from the rectangle of area ηz_0 .

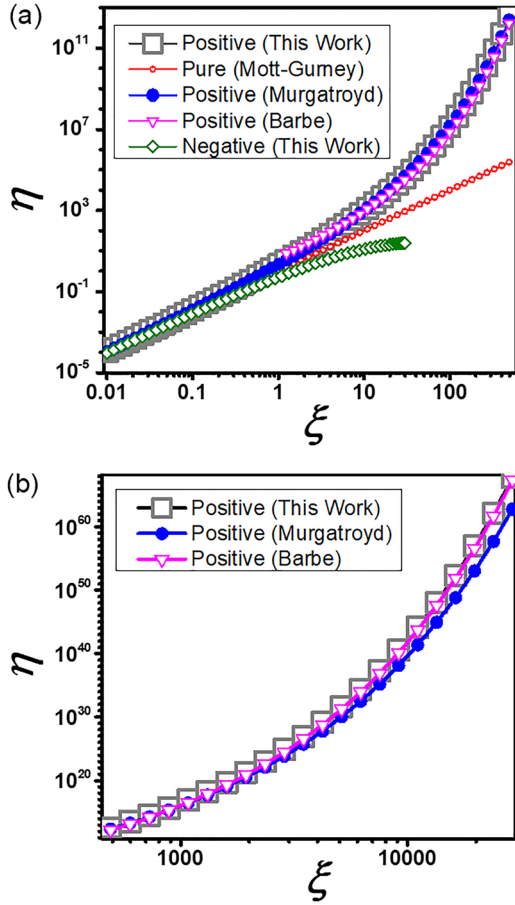


FIG. 2. Variation of normalized current density (η) against normalized applied voltage (ξ) obtained from the exact solution derived here in comparison to pure SCLC (Mott and Gurney), Murgatroyd's original solution, and Barbe's analytical solution for (a) $\xi < 500$ and (b) $\xi > 500$.

Figure 2 shows the variation of the normalized current η against the normalized voltage ξ for both positive and negative field dependence obtained using Eqs. (18) and (19) compared to data obtained using Murgatroyd's expression and Barbe's high-field approximation. As can be seen, at low electric field ($\xi < 1$, corresponding to ~ 4 kV/cm for a material with $\epsilon_r = 5$), the log-log plot of η against ξ yields a straight line with slope 2, consistent with the pure square-law dependence of the SCLC given by Mott and Gurney. Above $\xi \approx 1$ however, the current deviates significantly from the Mott-Gurney law. In comparing the exact values calculated here to Murgatroyd's and Barbe's treatments, we see that Murgatroyd's expression gives current-voltage data close to the exact values (within 11%) up to moderate electric field ($\xi < 100$, corresponding to < 0.4 MV/cm for a material with $\epsilon_r = 5$) [Fig. 2(a)] and remains the better choice as compared to Barbe's expression up to $\xi \approx 1000$ (corresponding to ~ 4 MV/cm for materials with $\epsilon_r = 5$). It is only above this field, which is in fact sufficiently high to cause dielectric breakdown in most materials, that Barbe's expression becomes closer to the exact one [Fig. 2(b)].

Because the carrier mobility/carrier concentration has an exponential relation with the square root of the electric field,

it is reasonable to check whether the same exponential relation holds for the normalized current and the square root of the normalized voltage applied. Figure 3 shows the variation of $\ln(\eta/\xi^2)$ versus $\sqrt{\xi}$. For both positive as well as negative field dependence, the data fit very closely to straight lines. However, at very high field, the data for the positive field dependence begin to deviate from linearity. Neglecting the small intercepts in the fit, the relation between η and ξ can be approximated closely as

$$\eta = \xi^2 \exp\left(0.727\sqrt{\xi}\right); \quad \text{for positive field dependence,} \quad (20a)$$

$$\eta = \xi^2 \exp\left(-0.654\sqrt{\xi}\right); \quad \text{for negative field dependence.} \quad (20b)$$

Equations (20a) and (20b) can now be converted to the relation between the current density and the applied voltage as

$$J = \frac{9}{8} \epsilon \mu_0 \frac{V^2}{d^3} \exp\left(0.891\gamma\sqrt{\frac{V}{d}}\right); \quad \text{for positive field dependence,} \quad (21a)$$

$$J = \frac{9}{8} \epsilon \mu_0 \frac{V^2}{d^3} \exp\left(-0.801\gamma\sqrt{\frac{V}{d}}\right); \quad \text{for negative field dependence.} \quad (21b)$$

The expression for positive field agrees with that reported by Murgatroyd and very closely represents the exact J - V data for a moderately high electric field. In the case of negative field dependence, the solution takes the same functional form as for positive field dependence but with a different exponential factor of -0.801 .

When using Murgatroyd's SCLC expression to probe the charge carrier mobility in disordered materials, one typically does not *a priori* know the nature (zero, positive, negative) of its electric field dependence. However, in the case of negative field dependence, the use of Murgatroyd's original

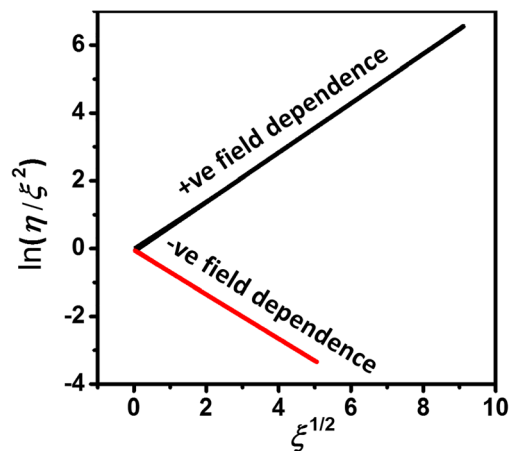


FIG. 3. Plotting the variation of $\ln(\eta/\xi^2)$ against $\sqrt{\xi}$ yields a straight line, which supports the exponential dependence of the normalized current (η) on the square root of the normalized voltage $\sqrt{\xi}$.

expression would be incorrect, and the expression derived here specifically for this case [Eq. (21b)] should instead be used. In order to accurately fit the data using SS-SCLC analysis, one must therefore first identify both the correct SCLC region to fit *and* the nature of the electric field dependence. If the test material exhibits field-dependent mobility, a traditional log–log analysis of the J – V data⁴ will not produce a straight line with slope 2. In particular, a material exhibiting negative field dependence would yield a region with slope less than 2, which can easily be overlooked without careful analysis. On the other hand, the natural transition between ohmic and space-charge-limited regimes in a log–log plot could possibly be mistaken as a region of negative field dependence. Therefore, a better approach is arguably to begin by plotting a graph of $\ln(J/E^2)$ against \sqrt{E} , which will yield a straight line with negative slope in the case of SCLC with negative field dependence and a straight line with positive slope in the case of SCLC with positive field dependence. A region of zero slope corresponds to SCLC with no field dependence. Independently, an investigation of the thickness dependence of the current–voltage behavior can confirm the existence of space-charge-limited current based on the expected inverse proportionality between current and thickness at constant V/d [Eqs. (21a) and (21b)].⁴ With this information in hand, one can then proceed to fit the appropriate region of the data with Eqs. (21a) and (21b) to obtain the desired charge transport parameters.

III. SUMMARY

We have extended the theory of space-charge-limited current with an exponential electric field dependence of mobility/carrier concentration, originally reported by Murgatroyd, for

the case of negative field dependence. Although the obtained current–voltage relations are based on fitting of the normalized current–normalized voltage ($\eta - \xi$) data similarly to Murgatroyd’s original work, here an exact integration procedure has been used in lieu of the inherently inexact numerical integration procedure originally applied by Murgatroyd. For the case of positive field dependence, the correct solution is compared with Murgatroyd’s numerical solution as well as with the analytical solution given by Barbe at high field. At low to moderately high field, Murgatroyd’s result is very close to the exact solution, and only at very high field does Barbe’s result begin to converge with the exact solution. In the case of negative field dependence, the current–voltage relation can be described by a function identical to that originally given by Murgatroyd, but with a different negative exponential factor of -0.801 . This newly derived equation can and should be applied to the steady-state current–voltage analysis of materials exhibiting negative-field-dependent mobility. Importantly, this development of steady-state space-charge-limited current analysis extends the utility of this technique to a greater range of challenging materials, and may provide an important tool for verifying transient results.

ACKNOWLEDGMENTS

This work has been supported by the Defense Threat Reduction Agency under Grant No. HDTRA1-15-1-0020 and in part by funds provided through the University of Missouri-Kansas City School of Graduate Studies Research Grant program.

APPENDIX: EVALUATION OF INTEGRAL / [EQ. (17)]

$$\begin{aligned}
 I &= z_0 \eta - \int_0^{z_0} \eta y(z) dz \\
 &= z_0 \left[24 + 4 \exp(\sqrt{z_0}) \left(z_0^{\frac{3}{2}} - 3z_0 + 6\sqrt{z_0} - 6 \right) \right] - 24z_0 - 4 \left[2 \exp(\sqrt{z_0}) \left(z_0^2 - 7z_0^{\frac{3}{2}} + 27z_0 - 60\sqrt{z_0} + 60 \right) - 120 \right] \\
 &= \exp(\sqrt{z_0}) \left(4z_0^{\frac{5}{2}} - 12z_0^2 + 24z_0^{\frac{3}{2}} - 24z_0 \right) - \exp(\sqrt{z_0}) \left(8z_0^2 - 56z_0^{\frac{3}{2}} + 216z_0 - 480\sqrt{z_0} + 480 \right) + 480 \\
 &= \exp(\sqrt{z_0}) \left(4z_0^{\frac{5}{2}} - 20z_0^2 + 80z_0^{\frac{3}{2}} - 240z_0 + 480\sqrt{z_0} - 480 \right) + 480 \\
 &= 4 \exp(\sqrt{z_0}) z_0^2 (\sqrt{z_0} - 5) + 20 \left[4 \exp(\sqrt{z_0}) \left(z_0^{\frac{3}{2}} - 3z_0 + 6\sqrt{z_0} - 6 \right) + 24 \right] \\
 &= 4 \exp(\sqrt{z_0}) \left(z_0^{\frac{5}{2}} - 5z_0^2 \right) + 20\eta.
 \end{aligned}$$

¹A. C. Arias, J. D. MacKenzie, I. McCulloch, J. Rivnay, and A. Salleo, *Chem. Rev.* **110**, 3 (2010).

²M. Kaltenbrunner, T. Sekitani, J. Reeder, T. Yokota, K. Kuribara, T. Tokuhara, M. Drack, R. Schwödauier, I. Graz, S. Bauer-Gogonea, S. Bauer, and T. Someya, *Nature* **499**, 458 (2013).

³C. Wang, H. Dong, W. Hu, Y. Liu, and D. Zhu, *Chem. Rev.* **112**, 2208 (2012).

⁴J. C. Blakesley, F. A. Castro, W. Kylberg, G. F. A. Dibb, C. Arantes, R. Valaski, M. Cremona, J. S. Kim, and J.-S. Kim, *Org. Electron.* **15**, 1263 (2014).

⁵A. Kokil, K. Yang, and J. Kumar, *J. Polym. Sci. Part B Polym. Phys.* **50**, 1130 (2012).

⁶R. P. Rocha and J. A. Freire, *J. Appl. Phys.* **112**, 083717 (2012).

⁷A. Many and G. Rakavy, *Phys. Rev.* **126**, 1980 (1962).

⁸G. Juška, K. Arlauskas, M. Viliūnas, and J. Kočka, *Phys. Rev. Lett.* **84**, 4946 (2000).

⁹M. A. Lampert and P. Mark, *Current Injection in Solids* (Academic Press, 1970).

¹⁰N. F. Mott and R. W. Gurney, *Electronic Processes in Ionic Crystals*, 2nd ed. (Oxford University Press, 1950).

¹¹A. Rose, *Phys. Rev.* **97**, 1538 (1955).

¹²G. González, *J. Appl. Phys.* **117**, 084306 (2015).

¹³J. Frenkel, *Phys. Rev.* **54**, 647 (1938).

¹⁴P. N. Murgatroyd, *J. Phys. D Appl. Phys.* **3**, 151 (1970).

¹⁵D. F. Barbe, *J. Phys. D Appl. Phys.* **4**, 1812 (1971).

¹⁶J. Bisquert, J. M. Montero, H. J. Bolink, E. M. Barea, and G. Garcia-Belmonte, *Phys. Status Solidi* **203**, 3762 (2006).

- ¹⁷H. Bässler, *Phys. Status Solidi* **175**, 15 (1993).
- ¹⁸A. J. Mozer and N. S. Sariciftci, *Chem. Phys. Lett.* **389**, 438 (2004).
- ¹⁹S. Raj Mohan, M. P. Joshi, and M. P. Singh, *Chem. Phys. Lett.* **470**, 279 (2009).
- ²⁰V. Kazukauskas, M. Pranaitis, V. Čyras, L. Sicot, and F. Kajzar, *Thin Solid Films* **516**, 8988 (2008).
- ²¹A. K. Tripathi and Y. N. Mohapatra, *Org. Electron.* **11**, 1753 (2010).
- ²²G. Juška, K. Genevičius, K. Arlauskas, R. Österbacka, and H. Stubb, *Phys. Rev. B* **65**, 233208 (2002).
- ²³A. Hirao, H. Nishizawa, and M. Sugiuchi, *Phys. Rev. Lett.* **75**, 1787 (1995).
- ²⁴A. Mozer, N. Sariciftci, A. Pivrikas, R. Österbacka, G. Juška, L. Brassat, and H. Bässler, *Phys. Rev. B* **71**, 035214 (2005).
- ²⁵S. D. Baranovskii, *Phys. Status Solidi* **251**, 487 (2014).
- ²⁶I. Fishchuk, A. Kadashchuk, H. Bässler, and M. Abkowitz, *Phys. Rev. B* **70**, 245212 (2004).
- ²⁷I. I. Fishchuk, A. Kadashchuk, and H. Bässler, *Phys. Status Solidi* **3**, 271 (2006).
- ²⁸O. J. Weiß, R. K. Krause, and A. Hunze, *J. Appl. Phys.* **103**, 043709 (2008).